



HAL
open science

Quantum walk hydrodynamics

Mohamed Hatifi, Giuseppe Di Molfetta, Fabrice Debbasch, Marc Brachet

► **To cite this version:**

Mohamed Hatifi, Giuseppe Di Molfetta, Fabrice Debbasch, Marc Brachet. Quantum walk hydrodynamics. Scientific Reports, 2019, 9 (1), pp.2989 (2019). 10.1038/s41598-019-40059-x . hal-02057635

HAL Id: hal-02057635

<https://hal.sorbonne-universite.fr/hal-02057635v1>

Submitted on 5 Mar 2019

HAL is a multi-disciplinary open access archive for the deposit and dissemination of scientific research documents, whether they are published or not. The documents may come from teaching and research institutions in France or abroad, or from public or private research centers.

L'archive ouverte pluridisciplinaire **HAL**, est destinée au dépôt et à la diffusion de documents scientifiques de niveau recherche, publiés ou non, émanant des établissements d'enseignement et de recherche français ou étrangers, des laboratoires publics ou privés.

SCIENTIFIC REPORTS

OPEN

Quantum walk hydrodynamics

Mohamed Hatifi¹, Giuseppe Di Molfetta^{2,3}, Fabrice Debbasch⁴ & Marc Brachet⁵

A simple Discrete-Time Quantum Walk (DTQW) on the line is revisited and given an hydrodynamic interpretation through a novel relativistic generalization of the Madelung transform. Numerical results show that suitable initial conditions indeed produce hydrodynamical shocks and that the coherence achieved in current experiments is robust enough to simulate quantum hydrodynamical phenomena through DTQWs. An analytical computation of the asymptotic quantum shock structure is presented. The non-relativistic limit is explored in the Supplementary Material (SM).

Received: 6 June 2018

Accepted: 22 November 2018

Published online: 27 February 2019

Quantum walks (DTQWs) are unitary quantum automata that can be viewed as formal generalizations of classical random walks. Following the seminal work of Feynman¹ and Aharonov² they were considered in a systematic way by Meyer³. DTQWs have been realized experimentally with a wide range of physical objects and setups^{4–10}, and are studied in a large variety of contexts, ranging from quantum optics¹⁰ to quantum algorithmics^{11,12}, solid-state physics^{13–16} and biophysics^{17,18}. The aim of this Letter is to show on a simple example, through both literal and numerical computations, that QW dynamics can be mapped onto quantum fluid dynamics (QFD) and that QWs can thus be used to model and experimentally simulate quantum fluids. In particular, DTQWs are thus natural candidates for future laboratory simulation of matter wave interferences in quantum fluids, dispersive hydrodynamics¹⁹ and extreme astrophysical plasmas (see e.g. §3.2.3 and §3.2.4 in²⁰).

We focus on a simple spatially homogeneous and time independent DTQW on the line whose continuous limit is identical to the free Dirac equation in flat 2D space-time. We then introduce a new relativistic generalization of the Madelung transform which maps this Dirac equation into a 2D dispersive hydrodynamics for relativistic quantum fluids. In the non relativistic limit, the two component spinor which obeys the Dirac equations degenerates into a single wave-function which obeys the Schrödinger equation, which can also be viewed as the continuous space limit of a continuous time quantum walk. The relativistic Madelung transform then becomes the usual Galilean Madelung transform. To prove that the hydrodynamical vision goes beyond a mere rewriting of the equations, we demonstrate through direct numerical simulations that the DTQW can actually model QFD shocks. We also present an analytical computation of the asymptotic Galilean shock structure through Pearcey integral commonly used in Optics.

Methods

The DTQW. The Hilbert space of the DTQW is the tensor product $\mathcal{H}_p \otimes \mathcal{H}_s$, where \mathcal{H}_p is the discrete line with basis $n, n \in \mathbb{Z}$ and \mathcal{H}_s is the ‘spin’-space with basis vectors $|L\rangle = (1, 0)^T$ and $|R\rangle = (0, 1)^T$. The evolution is controlled by the unitary operator $U = TC$, where $T = \sum_n [|n-1, L\rangle \langle n, L| + |n+1, R\rangle \langle n, R|]$ is the translation operator and $C = e^{-i\theta\sigma_1}$ is the quantum coin operator defined from the first Pauli matrix σ_1 and an arbitrary constant angle θ . The explicit evolution equation of the walk reads:

$$\begin{bmatrix} \Psi_L(l+1, n-1) \\ \Psi_R(l+1, n+1) \end{bmatrix} = \begin{bmatrix} \cos\theta & -i\sin\theta \\ -i\sin\theta & \cos\theta \end{bmatrix} \begin{bmatrix} \Psi_L(l, n) \\ \Psi_R(l, n) \end{bmatrix} \quad (1)$$

where the index l represents the iteration or discrete time.

Continuous Limit. Introduce now two positive real numbers m and ε , choose $\theta(\varepsilon, m) = \varepsilon m$, consider that $\Psi_{L/R}(l, n)$ are the values taken by some differentiable functions $\Psi_{L/R}(t, x)$ at point $t_l = l\varepsilon$ and $x_n = n\varepsilon$. Equation (1) then admits a continuous limit which coincides with the Dirac equation²¹

¹Aix-Marseille Université, CNRS, École Centrale de Marseille, Institut Fresnel UMR 7249, 13013, Marseille, France.

²Aix-Marseille Université, Université de Toulon, CNRS, LIS, France, Natural Computation research group, Marseille, France. ³Departamento de Física Teórica and IFIC, Universidad de Valencia-CSIC, Dr. Moliner 50, 46100, Burjassot, Spain. ⁴LERMA, UMR 8112, UPMC and Observatoire de Paris, 61 Avenue de l’Observatoire, 75014, Paris, France.

⁵Laboratoire de Physique Statistique, École Normale Supérieure, PSL Research University, UPMC Univ Paris 06, Sorbonne Universités, Université Paris Diderot, Sorbonne Paris-Cité, CNRS, 24 Rue Lhomond, 75005, Paris, France. Correspondence and requests for materials should be addressed to G.D.M. (email: giuseppe.dimolfetta@lis-lab.fr)

$$i\gamma^\mu \partial_\mu \psi - m\psi = 0, \tag{2}$$

where $\psi = (\Psi_L, \Psi_R)^T$, $\gamma^0 = \sigma_1$, $\gamma^1 = i\sigma_2$ (σ_2 is the second Pauli matrix) and $\hbar = c = 1$. The mass m is thus homogeneous to the inverse of a length.

Dirac Eq. (2) can be obtained from the Lagrangian density $\mathcal{L} = \frac{i}{2}(\bar{\psi}\gamma^\mu \partial_\mu \psi - \partial_\mu \bar{\psi}\gamma^\mu \psi) - m\bar{\psi}\psi$ where $\bar{\psi} = \psi^\dagger \gamma^0$. The associated particle current is $j^\mu = \bar{\psi}\gamma^\mu \psi$ and the stress energy tensor reads $T^{\mu\nu} = \frac{i}{4}[\bar{\psi}\gamma^\mu \partial^\nu \psi - \partial^\nu \bar{\psi}\gamma^\mu \psi + (\mu \leftrightarrow \nu)]$. Both j and T are conserved i.e. $\partial_\mu T^{\mu\nu} = 0$ and $\partial_\mu j^\mu = 0$. Note that the above Lagrangian density leads to a symmetric canonical stress-energy tensor.

Results

New variables. The definition of j leads to $j^0 = |\psi_R|^2 + |\psi_L|^2$ and $j^1 = |\psi_R|^2 - |\psi_L|^2$. Note that $(j^0)^2 - (j^1)^2 = 4|\psi_L|^2 |\psi_R|^2 \geq 0$ so that the current j is necessarily timelike or null. We then introduce $\varphi_\pm = \varphi_L \pm \varphi_R$ where $\varphi_{L/R}$ is the phase of $\Psi_{L/R}$ and replace the variables ($|\psi_L|^2, |\psi_R|^2, \phi_L, \phi_R$) by $(j^0, j^1, \varphi_+, \varphi_-)$. In particular, the spinor ψ now reads

$$\psi(\mathbf{x}, t) = \frac{1}{\sqrt{2}} e^{i\varphi_+/2} \begin{bmatrix} \sqrt{j^0 - j^1} e^{i\varphi_-/2} \\ \sqrt{j^0 + j^1} e^{-i\varphi_-/2} \end{bmatrix} \tag{3}$$

and $\varphi_+/2$ can be viewed as the global phase of ψ .

In terms if these new variables, the Lagrangian density and the stress energy tensor read $\mathcal{L} = -m(j_\mu j^\mu)^{1/2} \cos \varphi_- - \frac{1}{2}(j^\mu \partial_\mu \varphi_+ - \varepsilon^{\mu\nu} j_\nu \partial_\mu \varphi_-)$ and $T^{\mu\nu} = -\frac{1}{4}(j^\mu \partial^\nu \varphi_+ - \varepsilon^{\mu\alpha} j_\alpha \partial^\nu \varphi_- + (\mu \leftrightarrow \nu))$, where $\varepsilon^{\mu\nu}$ denotes the completely antisymmetric symbol of rank two, with the convention $\varepsilon^{01} = -\varepsilon^{10} = 1$.

The dynamical equations derived from $\mathcal{L}(j^0, j^1, \varphi_+, \varphi_-)$ are

$$e^\mu{}_\alpha \partial_\mu j^\alpha = 2m(j_\mu j^\mu)^{1/2} \sin \varphi_- \tag{4}$$

$$m \cos \varphi_- j^\mu = -\frac{1}{2}(j_\mu j^\mu)^{1/2} (\partial^\mu \varphi_+ + \varepsilon^{\mu\nu} \partial_\nu \varphi_-) \tag{5}$$

$$\partial_\mu j^\mu = 0. \tag{6}$$

Dirac quantum hydrodynamics. Since j is time-like or null, one can define the density n of the (1 + 1)D Dirac fluid by $n = (j_\mu j^\mu)^{1/2}$. We now suppose that j is not null and define the vector $u = j/n$ as the 2-velocity of the fluid, normed to unity. The two variables j^0 and j^1 can then be replaced by n and u^1 i.e. the density and the spatial part of the fluid 2-velocity. Equation (5) can then be re-written as $m \cos \varphi_- u^\mu = -\frac{1}{2}(\partial^\mu \varphi_+ + \varepsilon^{\mu\nu} \partial_\nu \varphi_-)$ and, in this form, brings to mind the standard relation $\frac{w}{n} u^\mu = -\partial^\mu \varphi$ which links the velocity u of a relativistic potential flow to its potential φ , the enthalpy per unit volume w and the particle density n . We thus retain $w = mn \cos \varphi_-$ as the enthalpy per unit volume of the (1 + 1)D Dirac fluid. The velocity field u then derives from two potentials. One is $\varphi_-/2$ i.e. the global phase of the spinor ψ and contributes to u in the standard way. The other potential is the phase differential $\varphi_-/2$ and contributes to u in a non-standard way, by contraction of its gradient with the (1 + 1)D completely antisymmetric symbol.

Using ((5)), one then finds that

$$T^{\mu\nu} = wu^\mu u^\nu + \frac{n}{2}(\varepsilon^{\mu\alpha} u_\alpha \partial^\nu \varphi_- + u^\mu \varepsilon^{\nu\alpha} \partial_\alpha \varphi_-), \tag{7}$$

to be compared with the stress-energy tensor $T^{\mu\nu} = wu^\mu u^\nu - p\eta^{\mu\nu}$ of a relativistic perfect fluid of pressure p . The pressure of the Dirac fluid thus vanishes. This is not surprising because classical pressure in spin-0 superfluids is generated by non-linearities²²⁻²⁴ in the wave equation and the free Dirac Eq. (2) is linear.

The last two terms on the right-hand side of (7) depend on the gradient of φ_- and, thus, on the gradient of w/n . Indeed, the definition of w leads to $\sin^2 \varphi_- = 1 - (\frac{w}{mn})^2$ and $\sin \varphi_- d\varphi_- = -d(\frac{w}{mn})$, so that, if $w \neq nm$,

$$\partial_\mu \varphi_- = -\sigma \frac{\partial_\mu (\frac{w}{mn})}{\left(1 - (\frac{w}{mn})^2\right)^{1/2}} \tag{8}$$

where σ is the sign of $\sin \varphi_-$. As for relativistic spin 0 superfluids²⁵, the two extra-terms in the above expression of the stress-energy tensor thus depend on the gradient of a thermodynamic function (the enthalpy per particle w/n) and are therefore best viewed as generalized ‘quantum pressure’ terms. As shown in the SM the two component spinor which obeys Dirac equation degenerates, in the Galilean limit, into a single wave-function which obeys the Schrödinger equation and the relativistic hydrodynamics degenerates into the standard²⁶⁻²⁸ Madelung hydrodynamics.

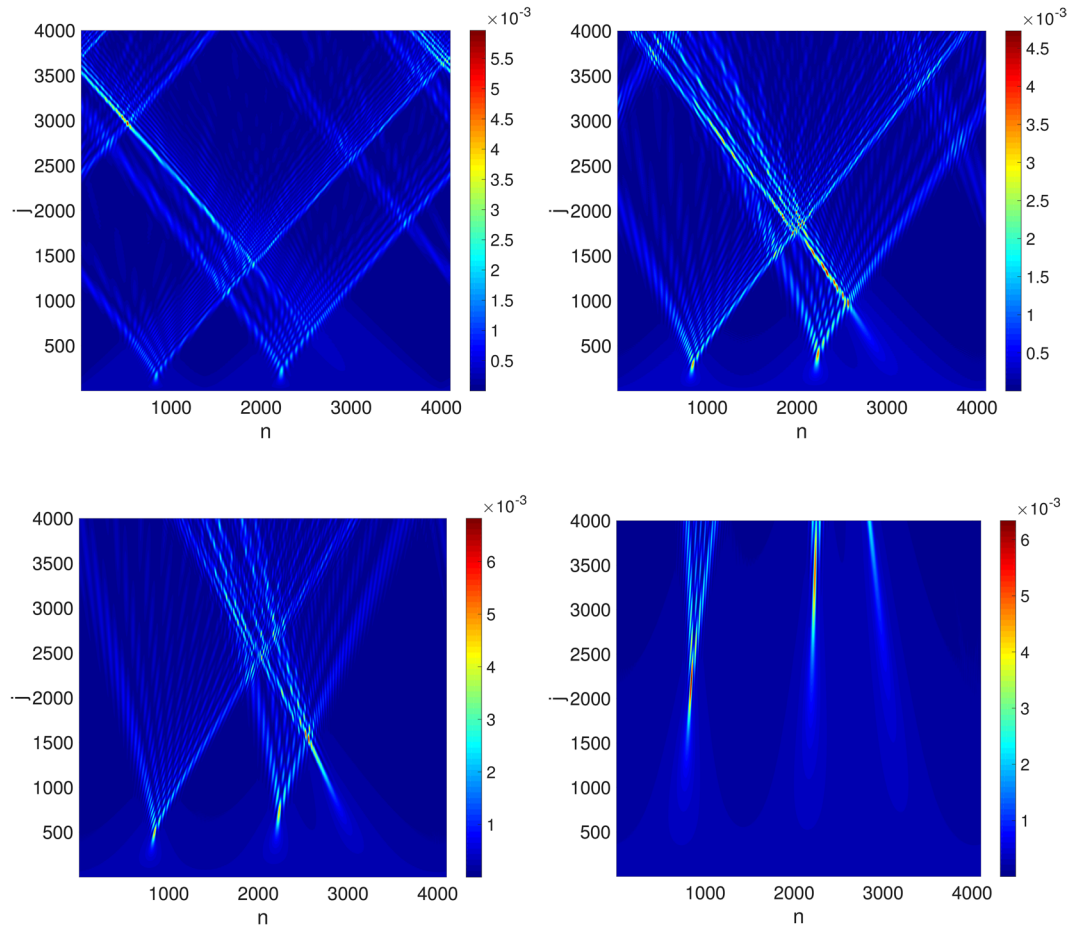


Figure 1. Unitary evolution of density $j^0 = |\Psi_L|^2 + |\Psi_R|^2$ for the DTQW defined in Eq. (1) with initial conditions: $\phi = q_{\max} [\cos(x) + \frac{1}{3} \cos(3x) + \frac{1}{2} \cos(2x + 0.9)]/m$ where $m := 25.6, 64, 128$ and $512, q_{\max} = 51.2$ and $u_{\max} = 2, 0.8, 0.4$ and 0.1 (see Eqs (9) and (10)). The grid has $N = 2^{12}$ points, $\varepsilon = 2\pi/N$.

Numerical shock simulation. The above generalization of the Madelung transform strongly suggests that the original DTQW can be used to simulate quantum flows. First note that a general positive energy plane wave solution of (2) can be written as (see (3–6)) $j^0 = n\sqrt{1 + q^2}, j^1 = nq, \varphi_+/2 = -m(\sqrt{1 + q^2}t - qx), \varphi_- = 0$, where q denotes both wave-number and momentum in unit of m (remember $\hbar = c = 1$). The spinor

$$\Psi_L = \sqrt{\sqrt{1 + q^2} - q} e^{im\phi/\sqrt{2}} \Psi_R = \sqrt{\sqrt{1 + q^2} + q} e^{im\phi/\sqrt{2}} \tag{9}$$

thus describes, at $t = 0$, a unit density fluid ($n = 1$) in motion with constant velocity u^1 given by $u^1 = q = \partial\phi/\partial x$. In order to simulate quantum flows, we now select the initial conditions of the form (9) but with

$$\phi = \frac{q_{\max}}{m} \left[\cos(x) + \frac{1}{3} \cos(3x) + \frac{1}{2} \cos(2x + 0.9) \right], \tag{10}$$

with $q_{\max} = mu_{\max}$ this choice corresponds to the velocity field $u^1 = u_{\max}(\sin(x) - \sin(3x) - \sin(2x + 0.9))$. These initial conditions are inspired by the similar (but somewhat simpler) choice $\phi = q_{\max} \cos(x)/m$ which has already been used in the cosmological context to simulate the dynamics of (i) a non-quantum cosmological fluid?, (ii) a Bose-Einstein condensates of axions? Figure 1 shows the evolution of the initial condition (10) through the DTQW for various values of m and constant q_{\max} (the larger the mass, the less relativistic the propagation) and displays multiple shocks. The evolution of (11) is shown in Fig. 2 (compare Fig. 2a,b), which displays a single symmetric shock. Thus, both figures reveal that the DTQW can indeed be used to simulate hydrodynamical shocks in a quantum fluid^{29,30}.

Let us stress that the shock is present, not only at high resolutions, but also for resolutions as low as $n = 64$ (see Fig. 2), which is well within current experimental limits^{31,32}.

Analytical shock computation in the Galilean regime. We now present an analytical computation which reproduces the shock solution in the Galilean limit where the DTQW becomes a continuous time quantum

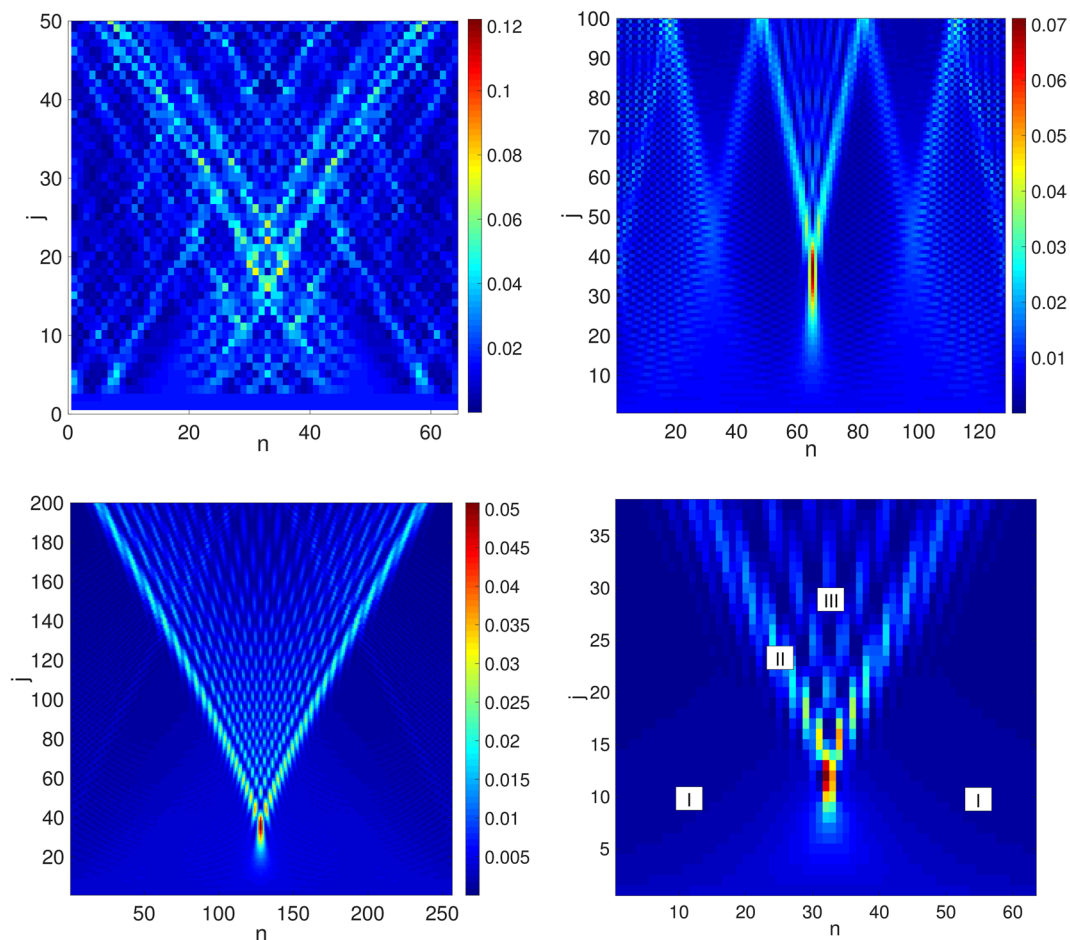


Figure 2. (a–c) DTQWs with initial conditions $\phi \sim \cos(x)$, $u_{\max} = 0.2$ and number of grid points $n = 64$ (a), $n = 128$ (b), $n = 256$ (c,d) Approximation by Pearcey’s integral in (x, t) space with $\varepsilon = 0.05$ and zones of validity of approximations (see text).

walk and the Dirac equation goes, as shown in the Supplemental Material, into the ($\hbar = 0$) Schrödinger equation $i\partial_t\psi = -\frac{1}{2m}\partial_{xx}\psi$.

The Green function for the Schrödinger equation reads

$$G_0(x, t|x_0, t_0) = \sqrt{\frac{m}{2i\pi(t-t_0)}} e^{\frac{im(x-x_0)^2}{2(t-t_0)}}. \tag{11}$$

The single-shock solution ($t_0 = 0$ and $u_{\max} = 1$) thus reads

$$\psi(\mathbf{x}, t) = \int_{-\infty}^{\infty} dy \sqrt{\frac{m}{2i\pi t}} e^{im\left(\frac{(y-x)^2}{2t} + \cos(y)\right)}. \tag{12}$$

In the large- m limit, this integral can be computed by making use of methods that are standard in optics³³ and involve Pearcey’s integral³⁴ defined by

$$I_{\mathcal{P}}(T, X) = \int_{-\infty}^{\infty} dy e^{i(Xy+Ty^2+y^4)}. \tag{13}$$

To wit, we set in the large- m limit, $\psi(\mathbf{x}, t) \approx A(\mathbf{x}, t)I_{\mathcal{P}}(-T(t), X(\mathbf{x}, t))$ with $T(t) = a^{-\frac{1}{2}}\left(\frac{t-1}{2\varepsilon t}\right)$, $X(\mathbf{x}, t) = -a^{-\frac{1}{4}}\left(\frac{x}{\varepsilon t}\right)$ and $A(\mathbf{x}, t) = e^{i\left(1+\frac{x^2}{2t}\right)/\varepsilon}(2i\pi t\varepsilon\sqrt{a})^{-1/2}$ where $a = m/4!$ and $\varepsilon = 1/m$. In this way, Pearcey’s integral Eq. (13) alone can correctly reproduce the structure of the shock (see Fig. 2c).

Useful asymptotic expansions of $I_{\mathcal{P}}$ are given in^{35,36} and §36.2 of³⁷. In particular, the steepest descent method can be directly used in zone I (see Fig. 2d) where $m \gg t/x^2$. It yields the the following asymptotic form:

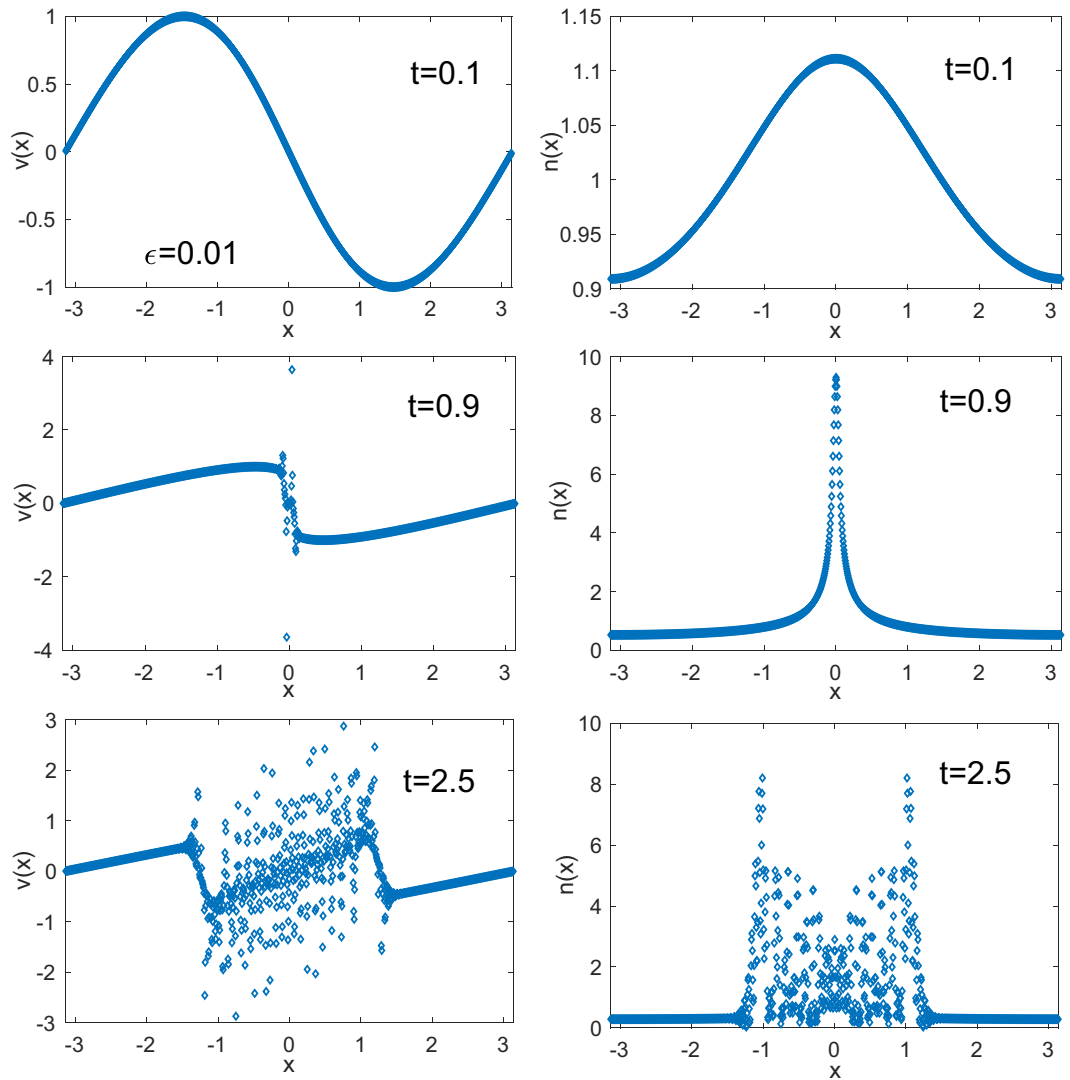


Figure 3. Evolution of velocity $v = m^{-1}\partial_x\varphi$ (left) and density n (right) for 3 values of time and $m^{-1} = 0.01$ obtained from a numerical solution of Schrödinger equation $i\partial_t\psi = -\frac{1}{2m}\partial_{xx}\psi$, with $\psi = n^{1/2}\exp i\varphi$ and initial conditions $\varphi = m\cos x$ and $n = 1$.

$$\psi_I(\mathbf{x}, t) \approx A(\mathbf{x}, t) \sqrt{\frac{-2i\pi}{\Phi''(u_c)}} e^{i\Phi(u_c)} \tag{14}$$

where $\Phi(u) = u^4 - Tu^2 + Xu$ and the single saddle-point u_c obeys $\Phi'(u_c) = 0$. Near the caustic, in zone II of Fig. 2d, 2 new saddle-points appear and the wavefunction can be written in terms of the Airy function $Ai(x) = \frac{1}{\pi} \int_{-\infty}^{\infty} dt \cos\left(\frac{t^3}{3} + xt\right)$. Well inside the caustic in zone III, the function can be written as the sum of 3 interfering contributions (see Fig. 2c,d).

Details of the evolution of the density $n = |\psi|^2$ and velocity $v = \partial_x\phi/m$ of the Schrödinger shock are presented in Fig. 3.

Conclusion

We have shown through a novel generalization of the Madelung transform that one of the simplest DTQWs on the line can be considered as a minimalist model of quantum fluids. This conclusion has been supported by numerical simulations which show that, even within the coherence limit of current experiments, the DTQW evolves an initial condition already considered in the literature into a quantum hydrodynamic shock^{29,30}. Thus, under current experimental conditions, DTQW can exhibit hydrodynamical behaviour and, therefore, be used to simulate quantum fluid dynamics. We have also computed the asymptotic shock structure analytically in the non-relativistic limit and proposed an extensive discussion of this limit in the SM.

Quantum walks have already been linked to with hydrodynamics in^{38,39}, but these earlier results address the quantum Boltzmann equation and transport phenomena, and are thus quite different from those presented in this Letter.

Note that the quantum fluid described in this article exhibits a non-vanishing quantum pressure but its traditional pressure vanishes identically because the underlying QW is linear. The results presented in this article can be generalised to quantum fluids with non vanishing traditional pressure by working with non-linear QWs such as those already considered in^{40–42}. The non-linearity of these walks can be reconciled with the linearity of Quantum Physics by viewing the non-linear terms as an effective description of (self-)interaction, generated for example by the coupling of QWs through gauge fields^{21,43–45}. Let us note that non-linear QWs can in principle be realized experimentally, at least through non-linear optics experiments^{46,47}.

The present work should be extended to higher dimensions and higher spins. Also, classical pressure terms should be added by considering non-linear DTQWs⁴¹, or DTQWs with site to site interactions. One should finally incorporate in the Madelung transform the natural coupling of DTQWs to gauge fields^{21,44,45,48}, thus obtaining novel models of superconducting quantum fluids or of quantum fluids in relativistic gravitational fields.

References

1. Feynman, R. & Hibbs, A. Quantum mechanics and path integrals. *International Series in Pure and Applied Physics* (McGraw-Hill Book Company, 1965).
2. Aharonov, Y., Davidovich, L. & Zagury, N. Quantum random walks. *Phys. Rev. A* **48**, 1687–1690, <https://doi.org/10.1103/PhysRevA.48.1687> (1993).
3. Meyer, D. A. From quantum cellular automata to quantum lattice gases. *Journal of Statistical Physics* **85**, 551–574, <https://doi.org/10.1007/BF02199356> (1996).
4. Schmitz, H. *et al.* Quantum walk of a trapped ion in phase space. *Phys. Rev. Lett.* **103**, 090504, <https://doi.org/10.1103/PhysRevLett.103.090504> (2009).
5. Zähringer, F. *et al.* Realization of a quantum walk with one and two trapped ions. *Phys. Rev. Lett.* **104**, 100503 (2010).
6. Schreiber, A. *et al.* Photons walking the line: A quantum walk with adjustable coin operations. *Phys. Rev. Lett.* **104**, 050502, <https://doi.org/10.1103/PhysRevLett.104.050502> (2010).
7. Karski, M. *et al.* Quantum walk in position space with single optically trapped atoms. *Science* **325**, 174–177, <https://doi.org/10.1126/science.1174436> (2009).
8. Sansoni, L. *et al.* Two-particle bosonic-fermionic quantum walk via integrated photonics. *Phys. Rev. Lett.* **108**, 010502, <https://doi.org/10.1103/PhysRevLett.108.010502> (2012).
9. Sanders, B., Bartlett, S., Tregenna, B. & Knight, P. Two-particle bosonic-fermionic quantum walk via 3d integrated photonics. *Phys. Rev. A* **67**, 042305 (2003).
10. Perets, B. *et al.* Realization of quantum walks with negligible decoherence in waveguide lattices. *Phys. Rev. Lett.* **100**, 170506 (2008).
11. Ambainis, A. Quantum walk algorithm for element distinctness. *SIAM Journal on Computing* **37**, 210–239 (2007).
12. Magniez, F., A. Nayak, J. R. & Santha, M. Search via quantum walk. *SIAM Journal on Computing - Proceedings of the thirty-ninth annual ACM symposium on Theory of computing* (New York, ACM, 2007).
13. Aslangul, C. Quantum dynamics of a particle with a spin-dependent velocity. *Journal of Physics A: Mathematical and Theoretical* **38**, 1–16 (2005).
14. Bose, S. Quantum communication through an unmodulated spin chain. *Phys. Rev. Lett.* **91**, 207901 (2003).
15. Burgarth, D. Quantum state transfer with spin chains. *University College London PhD thesis* (2006).
16. Bose, S. Quantum communication through spin chain dynamics: an introductory overview. *Contemporary Physics* **48**, 13–30, <https://doi.org/10.1080/00107510701342313> (2007).
17. Collini, E. *et al.* Coherently wired light-harvesting in photosynthetic marine algae at ambient temperature. *Nature* **464** (2010).
18. Engel, G. S. *et al.* Evidence for wavelike energy transfer through quantum coherence in photosynthetic systems. *Nature* **446**, 782–786 (2007).
19. Hofer, M., Engels, P. & Chang, J. Matter-wave interference in bose-einstein condensates: A dispersive hydrodynamic perspective. *Physica D: Nonlinear Phenomena* **238**, 1311–1320, <https://doi.org/10.1016/j.physd.2008.08.021>, *Nonlinear Phenomena in Degenerate Quantum Gases* (2009).
20. Uzdensky, D. A. & Rightley, S. Plasma physics of extreme astrophysical environments. *Reports on Progress in Physics* **77**, 036902 (2014).
21. Molfetta, G. D., Brachet, M. & Debbasch, F. Quantum walks in artificial electric and gravitational fields. *Physica A: Statistical Mechanics and its Applications* **397**, 157–168, <https://doi.org/10.1016/j.physa.2013.11.036> (2014).
22. Nore, C., Brachet, M. & Fauve, S. Numerical study of hydrodynamics using the nonlinear schrödinger equation. *Physica D: Nonlinear Phenomena* **65**, 154–162, [https://doi.org/10.1016/0167-2789\(93\)90011-O](https://doi.org/10.1016/0167-2789(93)90011-O) (1993).
23. Nore, C., Abid, M. & Brachet, M.-E. Decaying Kolmogorov turbulence in a model of superflow. *Phys. Fluids* **9**, 2644–2669 (1997).
24. Dalfovo, F., Giorgini, S., Pitaevskii, L. P. & Stringari, S. Theory of Bose-Einstein condensation in trapped gases. *Rev. Mod. Phys.* **71** (1999).
25. Debbasch, F. & Brachet, M. Relativistic hydrodynamics of semiclassical fluids. *Physica D* **82**, 255 (1995).
26. Madelung, E. Eine anschauliche deutung der gleichung von schrödinger. *Naturwissenschaften* **14**, 1004–1004, <https://doi.org/10.1007/BF01504657> (1926).
27. Madelung, E. Quantentheorie in hydrodynamischer form. *Zeitschrift für Physik* **40**, 322–326, <https://doi.org/10.1007/BF01400372> (1927).
28. Donnelly, R. J. *Quantized Vortices in Helium II* (Cambridge University Press, 1991).
29. Hofer, M. A. *et al.* Dispersive and classical shock waves in bose-einstein condensates and gas dynamics. *Phys. Rev. A* **74**, 023623, <https://doi.org/10.1103/PhysRevA.74.023623> (2006).
30. Wan, W., Jia, S. & Fleischer, J. W. Dispersive superfluid-like shock waves in nonlinear optics. *Nat Phys* **3**, 46–51 (2007).
31. Boutari, J. *et al.* Large scale quantum walks by means of optical fiber cavities. *Journal of Optics* **18**, 094007 (2016).
32. Regensburger, A. *et al.* Photon propagation in a discrete fiber network: An interplay of coherence and losses. *Physical review letters* **107**, 233902 (2011).
33. Berry, M. V. & Klein, S. Colored diffraction catastrophes. *Proceedings of the National Academy of Sciences* **93**, 2614–2619 (1996).
34. Pearcey, T. Xcxi. the structure of an electromagnetic field in the neighbourhood of a cusp of a caustic. *The London, Edinburgh, and Dublin Philosophical Magazine and Journal of Science* **37**, 311–317, <https://doi.org/10.1080/14786444608561335> (1946).
35. Kaminski, D. Asymptotic expansion of the pearcey integral near the caustic. *SIAM Journal on Mathematical Analysis* **20**, 987–1005, <https://doi.org/10.1137/0520066> (1989).
36. López, J. L. & Pagola, P. J. The pearcey integral in the highly oscillatory region. *Applied Mathematics and Computation* **275**, 404–410, <https://doi.org/10.1016/j.amc.2015.11.080> (2016).
37. NIST Digital Library of Mathematical Functions. <http://dlmf.nist.gov/>, Release 1.0.17 of, Olver, F. W. J. *et al.* eds (12-22-2017).

38. Succi, S., Fillion-Gourdeau, F. & Palpacelli, S. Quantum lattice boltzmann is a quantum walk. *EPJ Quantum Technology* **2**, 1–17, <https://doi.org/10.1140/epjqt/s40507-015-0025-1> (2015).
39. Mezzacapo, A. *et al.* Quantum simulator for transport phenomena in fluid flows. *Scientific Reports* **5**, 13153, <https://doi.org/10.1038/srep13153> (2015).
40. Shikano, Y., Wada, T. & Horikawa, J. Discrete-time quantum walk with feed-forward quantum coin. *Scientific reports* **4**, 4427 (2014).
41. Di Molfetta, G., Debbasch, F. & Brachet, M. Nonlinear optical galton board: Thermalization and continuous limit. *Phys. Rev. E* **92**, 042923, <https://doi.org/10.1103/PhysRevE.92.042923> (2015).
42. Vakulchyk, L., Fistul, M., Qin, P. & Flach, S. Nonlinear disordered discrete time quantum walks. *Bulletin of the American Physical Society* (2018).
43. Márquez-Martín, I., Arnault, P., Di Molfetta, G. & Pérez, A. Electromagnetic lattice gauge invariance in two-dimensional discrete-time quantum walks. *Physical Review A* **98**, 032333 (2018).
44. Arnault, P., Di Molfetta, G., Brachet, M. & Debbasch, F. Quantum walks and non-abelian discrete gauge theory. *Phys. Rev. A* **94**, 012335, <https://doi.org/10.1103/PhysRevA.94.012335> (2016).
45. Arnault, P. & Debbasch, F. Quantum walks and discrete gauge theories. *Phys. Rev. A* **93**, 052301, <https://doi.org/10.1103/PhysRevA.93.052301> (2016).
46. Lee, C.-W., Kurzyński, P. & Nha, H. Quantum walk as a simulator of nonlinear dynamics: Nonlinear dirac equation and solitons. *Physical Review A* **92**, 052336 (2015).
47. Javadi, A. *et al.* Single-photon non-linear optics with a quantum dot in a waveguide. *Nature communications* **6**, 8655 (2015).
48. Arnault, P. & Debbasch, F. Quantum walks and gravitational waves. *Annals of Physics* **383**, 645–661, <https://doi.org/10.1016/j.aop.2017.04.003> (2017).

Author Contributions

Author's individual contribution: M.H., G.D.M., M.B. and F.D. wrote the main manuscript text and G.D.M. prepared Figures 1–3.

Additional Information

Supplementary information accompanies this paper at <https://doi.org/10.1038/s41598-019-40059-x>.

Competing Interests: The authors declare no competing interests.

Publisher's note: Springer Nature remains neutral with regard to jurisdictional claims in published maps and institutional affiliations.



Open Access This article is licensed under a Creative Commons Attribution 4.0 International License, which permits use, sharing, adaptation, distribution and reproduction in any medium or format, as long as you give appropriate credit to the original author(s) and the source, provide a link to the Creative Commons license, and indicate if changes were made. The images or other third party material in this article are included in the article's Creative Commons license, unless indicated otherwise in a credit line to the material. If material is not included in the article's Creative Commons license and your intended use is not permitted by statutory regulation or exceeds the permitted use, you will need to obtain permission directly from the copyright holder. To view a copy of this license, visit <http://creativecommons.org/licenses/by/4.0/>.

© The Author(s) 2019